2017

Subsurface transport in a North Inlet, South Carolina salt marsh: A porewater salinity model

Carolyn Ryan
University of South Carolina

Subsurface transport in a North Inlet, South Carolina salt marsh: A porewater salinity model

by

Carolyn Ryan

Bachelor of Science
Brigham Young University, 2013

Submitted in Partial Fulfillment of the Requirements

For the Degree of Master of Science in

Geological Sciences

College of Arts and Sciences

University of South Carolina

2017

Accepted by:

Alicia Wilson, Director of Thesis

James Morris, Reader

George Voulgaris, Reader

Cheryl L. Addy, Vice Provost and Dean of the Graduate School

ACKNOWLEDGEMENTS

I would like to thank Dr. Michael Myrick and Stefan Faulkner from University of South Carolina's Department of Chemistry and Biochemistry for their help with the spectroscopy and the quantification of fluorescein concentrations.

ABSTRACT

Subsurface transport in coastal salt marshes influences the nutrient budget of coastal environments, but is not fully understood. To expand our understanding of this transport, a simple numerical model was developed. The model simulated vertical transport of salt through the surficial muds at a North Inlet marsh on the coastal plain of South Carolina. To improve the model, a tracer study was utilized to calculate the average velocity of groundwater flow through the system. The model was compared with porewater salinity measured using tension samplers and passive diffusion samplers. Each method produced different, uncorrelated results. However, accounting for macro-pores in the surficial sediments may explain the differences. Some methods, including those utilizing tension samplers, mostly measure transport occurring in the macro-pores. Passive diffusion samplers and basic single-domain transport models may more closely represent transport through the matrix of the marsh. To understand subsurface transport across the whole marsh, both pore regimes need to be considered.

TABLE OF CONTENTS

LIST OF TABLES

LIST OF FIGURE

LIST OF SYMBOLS

C	Concentration of a tracer
$\bar{c}$	Time weighted average
C_0	Initial concentration, concentration at time of injection
c_i	Salinity concentration produced by a model at time step *i*
D_I	Longitudinal dispersivity
D_{II}	Transverse dispersivity
i	Number of time steps since the first time step used in the calculation
L	Displacement in the direction of flow
N	Unit area
n	Number of time steps used in the calculation for which a salinity concentration was calculated and recorded
r	Pearson correlation coefficient
t	Time since injection
u	uniform flow velocity
x	distance from injection site, perpendicular to flow
x_0	injection location, perpendicular to flow
z	distance from injection site, parallel to flow
z_0	injection depth
α	inverse capillary rise
σ_x	transverse dispersion constant of the system

σ_z longitudinal dispersion constant of the system

List of Abbreviations

CO-OPS ..... Center for Operational Oceanographic Products and Services

ET ..... Evapotranspiration

ITRC ..... Interstate Technology Regulatory Council

NERRS ..... National Estuarine Research Reserve System

NOAA ..... National Oceanic and Atmospheric Administration

TS1 ..... Tension sampler at location 1

TS2 ..... Tension sampler at location 2

USGS ..... United States Geological Society

VOC ..... Volatile organic compound

CHAPTER 1 INTRODUCTION

Subsurface transport in coastal salt marshes affects the productivity of the marsh and the adjacent coastal ocean. Within the marsh, transport of nutrients and salts by groundwater influences the type and productivity of plants found in the salt marsh (Howes et al., 1986; Gardner and Reeves, 2002). Groundwater discharging to tidal creeks at low tide contains more nutrients than the surface water (Whiting and Childers, 1989). The enriched groundwater transports nutrients to the coastal ocean, either through creeks or submarine discharge (Moore, 1999; Moore et al., 2002).

The timing and path of transport determines which biogeochemical reactions occur. In salt marsh sediments, nitrate-nitrogen from the surface water is transformed into ammonium before being exported to the estuary (Wilson and Morris, 2012). Some salt marsh halophytes transform toxic metal pollutants into nontoxic forms (Weis and Weis, 2004). *Spartina alterniflora*, for example, detoxifies inorganic selenium compounds (Ansede et al., 1999). For some pollutants, remediation is more efficient in sediments experiencing tidal variations than in permanently flooded sediments (Catallo and Junk, 2003). Knowledge of the timing and path of the transport of nutrients and pollutants through the marsh sediments is critical for understanding their impact on ecosystems in coastal waters.

Models of salt transport can increase our understanding of subsurface transport in salt marshes. Modeling porewater salinity enables the testing of transport mechanisms without needing to include complex biogeochemical reactions. Salt, a conservative

tracer, occurs naturally throughout the marsh in concentrations that are easily measured. Porewater salinity is also important because it impacts primary productivity (Mitsch and Gosselink, 2007).

Morris (1995) presented a mass balance model of porewater salinity in the top 30 cm of marsh sediments, where concentration over that depth was assumed to be uniform. Physical parameters are also uniform across the model's domain (Morris, 1995). Transport occurred by the means of infiltration of precipitation and flood water, gravity-driven groundwater flow, evapotranspiration, biological salt secretion, and diffusion (Morris, 1995). Good agreement between the model and observed salinities was achieved by using observed meteorological conditions and surface salinity measurements.

Wang et al. (2007) expanded the model from Morris (1995) horizontally to model the soil salinity throughout the intertidal zone. Physical characteristics were derived from field soil samples and averaged across the domain (Wang et al. 2007) using the approach Samardzioska and Popov (2005) described as the equivalent continuum representation. The modeled salinity responded to changes in ET, temperature, hydraulic conductivity, and bulk surface resistance to water vapor (Wang et al. 2007). The model agreed well with field observations (Wang et al. 2007).

The intent of this study was to produce a process-based model for estimating the salinity profile of porewater in the top meter of surficial sediments of a coastal salt marsh.

1.1 Conceptual model

Most salt marshes in the southeastern United States consist of low permeability muds overlying high permeability sands (Weigert and Freeman, 1990). The permeability of the top 20-30 cm of mud is increased by bioturbation. *Spartina alterniflora* roots and

crab burrows typically occupy this zone. The mud pinches out at the uplands leaving the sand exposed.

General trends in groundwater flow are driven by topographic differences, though tidal cycles also influence flow (Fig. 1.1). Rain infiltrates more readily in the sandy uplands than on the marsh. The infiltration forms a freshwater lens flowing down to the ocean. Tidal signals propagate through the sands. Receding tidal signals enhance ocean-wards flow, while the rising tide opposes the flow. The expression of these forces are different in the mud layer. In the mud, flow is almost exclusively vertical (Wilson and Morris, 2012). Receding tides invoke gravitational drainage as porewater drains from the mud to the sand. The exposed mud may lose a small amount of water to ET or gain a small amount to precipitation. When the mud is flooded by a rising tide, sea water infiltrates until the system is saturated. Upon saturation, no other flow can occur.

Transport by advection and dispersion introduces and removes salt from the marsh's porewater. Salt enters the system with the infiltrating seawater. Gravity drainage removes salt. Other processes, such as infiltrating precipitation, may alter the concentration of salts or cause transport within the system.

1.2 Field site

The study was conducted in a *Spartina alterniflora*-dominated salt marsh in coastal South Carolina (Fig. 1.2). The study site is in the North Inlet estuary at Georgetown, South Carolina, an area designated as a National Estuarine Research Reserve System (NERRS) site. The marsh, located on Goat Island (33°19.88'N, 79°11.87'W), has negligible hydraulic connection to the uplands. The marsh experiences semidiurnal tides with a mean range of 1.5 m (Gardner and Porter, 2001). The sampling

site has an elevation near mean high tide (Morris, 1995). The tide inundates the sampler location up to twice a day. Seasonal variations in tides decrease flooding frequency during the winter.

The marsh has a layer of organic-rich mud overlying a fine-grained, well-sorted sand typical of salt marshes in the southeastern United States (Weigert and Freeman, 1990; Gardner and Porter, 2001). In the high marsh, the surficial soils contain mostly sand-sized particles with 10% fine particles and 8% macro-organics (Bradley and Morris, 1990). Extensive bioturbation has resulted in a gradational increase in sand content with depth (Gardner and Porter, 2001). Bioturbation resulting from crab burrows create macro-pores extending downward to 20 cm below the marsh surface.

Meteorological and water quality data are measured nearby at Clambank and Oyster Landing monitoring station (Fig. 1.2). Water depth, surface water salinity, and water temperature data from the NERRS Clambank station and precipitation rates from the NERRS Oyster Landing station (http://cdmo.baruch.sc.edu/get/export.cfm) were used in this study. Supplemental water height data came from the Center for Operational Oceanographic Products and Services (CO-OPS; https://tidesandcurrents.noaa.gov/waterlevels.html?id=8662245) at Oyster Landing.

Sampling of porewater nutrients at Goat Island began in December 1993 and are still underway (Morris et al., 2013). Three passive diffusion samplers are permanently installed in the high marsh. Each location has samplers at 10 cm, 25 cm, 50 cm, 75 cm, and 100 cm below the marsh surface. The samplers equilibrate for a month before being removed for analysis (Morris et al., 2013). The samples are analyzed for major nutrients,

chloride, sulfide, and, since 2003, iron (II). Porewater nutrient data is published online at http://www.baruch.sc.edu/biological-databases (Morris et al., 2013).

Hughes et al. (2012) studied the connection between salinity measured by passive diffusion samplers and changes in salt marsh hydrology in another North Inlet marsh. They reported correlations between soil salinity and precipitation, ET, surface water salinity, and the frequency of non-inundating high tides (Hughes et al., 2012). The significance of these correlations varies throughout the year (Hughes et al., 2012). Hughes et al. (2012) also found that porewater 10 cm below the marsh surface was fresher than porewater at or below 25 cm depth.

This study aims to increase understanding of transport at Goat Island through field observations, a dye tracer study, and a numerical model. Goat Island was chosen because of the long-term monitoring of porewater at the site.

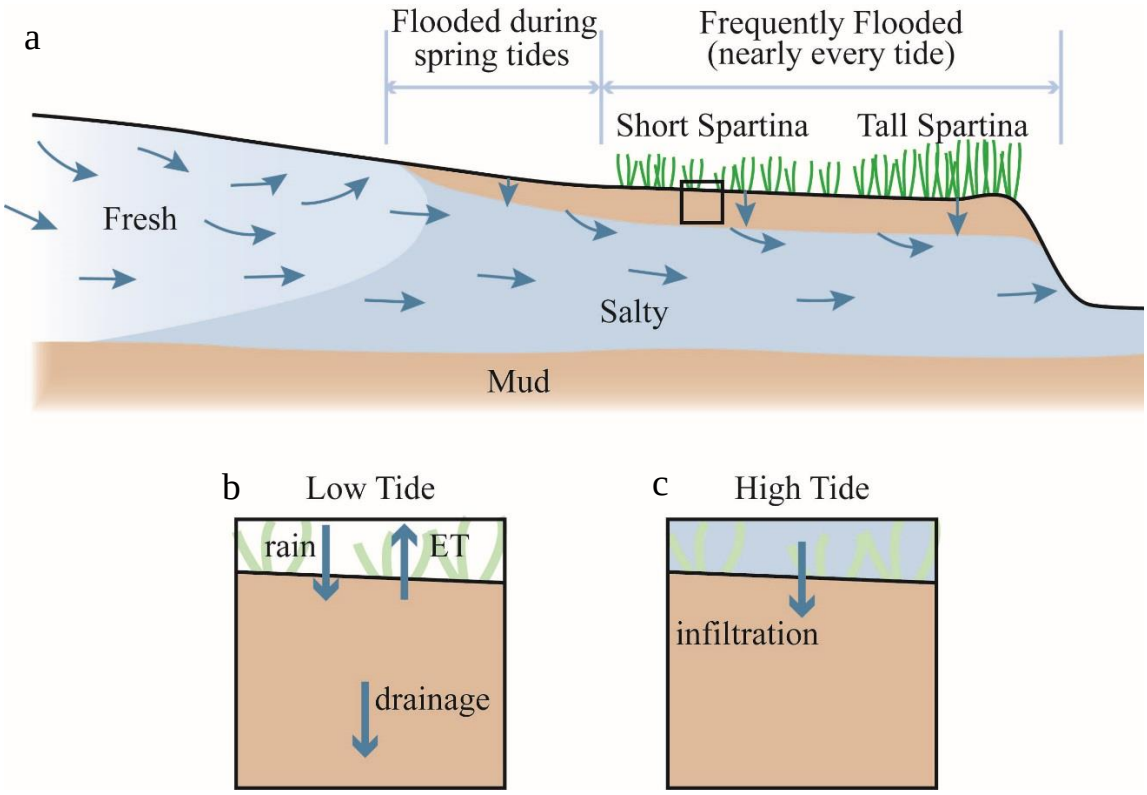

Figure 1.1 Conceptual model of groundwater flow in a coastal salt marsh. (a) Groundwater flow through salt marsh sediments. Arrows indicate the direction of groundwater flow. Black box indicates location of panels (b) and (c). (b) Groundwater flow when the marsh surface is exposed. (c) Groundwater flow when the marsh is inundated.

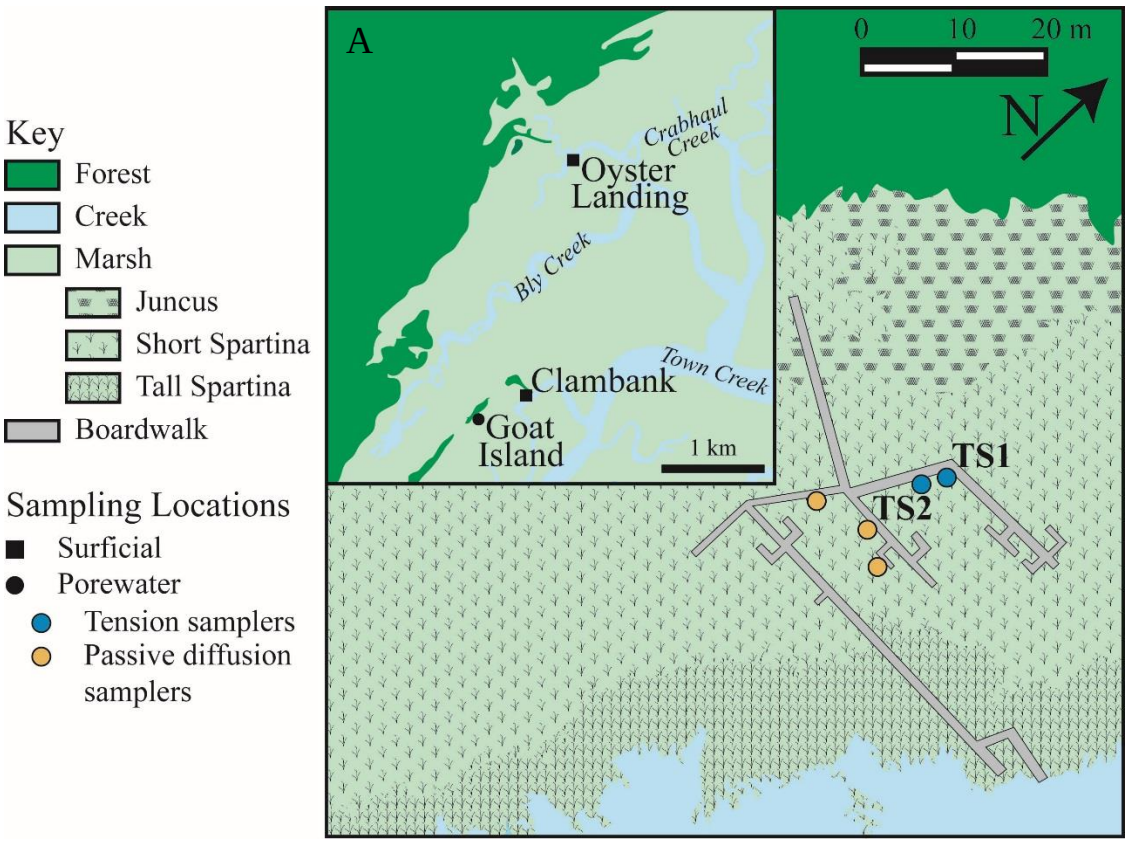

Figure 1.2 Data collection sites at Goat Island, North Inlet salt marsh, Georgetown, South Carolina. Circles indicate the location of porewater sampling. Tension samplers were used in the two northern locations (blue). Passive diffusion samplers are at the three other sites (yellow). The inset map (A) shows the location of Goat Island, indicated by a black circle, in the marsh at North Inlet. The squares indicate the surficial data collection stations.

CHAPTER 2 METHODS

2.1 Dye tracer study

A fluorescein tracer was used at two locations in the Goat Island high marsh. The deployment locations were equal distances from the tidal creek and roughly aligned with the permanent passive diffusion samplers (Fig. 1.2). To minimize sampler and tracer interactions, the locations were separated by 5 m. Different methods and depths of injection were used at each site. At the northern site, TS1, 1 mL of 848 g/L fluorescein was injected through a Rhizon deployed 5-15 cm below the marsh surface. Three milliliters of 848 g/L fluorescein were injected into a crab burrow at the southern location, TS2. The depth of this injection is assumed to be 0 cm.

2.1.1 Porewater sampling

Fluorescein concentrations were measured by taking porewater samples from depths of 10 cm, 25 cm, 50 cm, and 75 cm twice a week from February 7, 2017 to March 7, 2017. A total of 42 samples were collected. Samples were collected using Rhizon SMS samplers and push-point samplers. Both samplers relied on a 20 mL syringe to induce suction.

The Rhizons sampled porewater at 10 cm and 25 cm below the marsh surface. The samplers have a 2.5 mm diameter, a 10 cm porous interval, and a 0.15 μm mean pore size. Rhizon samplers were installed and left in place for the duration of the study. To improve control of the deployment depth with minimal disturbance to the sediments, the Rhizons were supported by a thin, rigid metal rod. For each location, two Rhizons were

attached to a rod such that the porous interval would be centered at the depths of interest after installation. Sampler installation consisted of inserting the prepared rod into the marsh sediments. The soft sediments allowed installation by hand without any extra tools. The vinyl tubing connected to each Rhizon is closed and held above the marsh surface between sampling.

The push-point sampled porewater from 50 and 75 cm below the marsh surface. The push-point has a 5 mm diameter and a 4 cm long slotted screen. The samples were collected within 20 cm of the Rhizon samplers.

Sampling began within two hours of the falling tide exposing the site and finished within 3.5 hours. All of the Rhizons were constantly sampling throughout this period. Two replicate samples were taken at each site. The first was thrown out as a purge. Sampling ended when 30 mL of porewater was removed or when the maximum suction failed to produce more porewater. Up to 50 mL of porewater was removed with the push-point to account for the additional filtration required before analyzing for chemical components.

Porewater samples collected with the push-point required filtering prior to further analysis. Rhizon samples do not need additional filtration because the small pore size excludes particulates. Before filtering, sediments in the sample were allowed to settle for at least 3 hours. The sample was decanted and checked for remaining sediment. If sediment was still visible, the process was repeated. Once the sample was clear, it was run through a coffee filter to finish processing.

2.1.2 Chemical analysis

Fluorescein concentrations were measured with a Cary 5000 UV-Vis spectrophotometer or a Hitachi Fluorescence Spectrophotometer F-4500. Highly concentrated samples, identified by a clear yellow color, were measured in the UV-Vis spectrophotometer. Samples with concentrations above the instrument's range were diluted. Less concentrated samples were measured with the fluorescence spectrophotometer. The results were compared with standards to calculate the sample's concentration.

2.1.3 Analytical model

An analytical solution of the advection-dispersion equation modeled fluorescein transport in the marsh. The solution, derived by DeJosselin De Jong (1958) and empirically verified by Bear (1961), assumes a slug injection into a two-dimensional, uniform flow field. The solution describes the concentration, *C*, of a tracer injected into this system at time *t* and location *(x, z)*, dependent on the velocity of flow, *u*, and the longitudinal and transverse dispersivities, D_I and D_{II} respectively. Using a version adapted from Bear (1961),

$$C(x,z,u,t) = \frac{C_0 N}{4\pi\sigma_z\sigma_x} exp\left[-\frac{\left(z-(z_0+ut)\right)^2}{2{\sigma_x}^2} - \frac{(x-x_0)^2}{2{\sigma_x}^2}\right]$$

where C_0 is the original concentration of the tracer injected at point (x_0, z_0), *N* is a unit area, and *u* represents the uniform flow velocity. The dispersivities are converted to the standard deviations of concentration in the system, σ_z and σ_x, by the equations $\sigma_z = \sqrt{2D_I L}$ and $\sigma_x = \sqrt{2D_{II} L}$ (Bear, 1961). Transverse dispersion occurred linearly in the model instead of radially, as it would in a three-dimensional system. As a result, the

transverse dispersivity used in the model is much larger than the actual dispersivity. Note that the 2D approximation only affects the degree of spreading, not the center of mass of the solute plume. Thus velocity estimates, which depend on the center of mass, are not affected by the 2D approximation.

The flow velocity, *u*, was estimated using the observed fluorescein concentrations. The solution assumes a constant groundwater velocity throughout the system that does not change over the represented period. For the data to be useful for calibrations, the samples must originate from a similar system. The average flow field needs to be temporally and spatially constant. The flow field near the surface of the marsh varies due to ET, precipitation, and tidal flooding. However, at greater depths, the effects of surface phenomena are smoothed, resulting in a fairly uniform flow field between tidal flooding. This smoothing allows the two deeper samples, taken at 50 cm and 75 cm below the marsh surface, to be used in the calibrations.

Table 2.1 lists the parameters used in the analytical model.

2.2 Salinity

2.2.1 Porewater sampling

The fluorescein samples were also analyzed for salinity. Salinity was measured with a YSI EcoSense EC300 Instrument using a four-electrode cell. The EC300 reported temperature compensated values. If sample size prevented an accurate measurement, the sample was diluted to an appropriate volume.

The salinity of the fluorescein samples, which were taken using tension samplers, were compared to the salinity measured by the passive diffusion samplers. Note that the two methods sample different populations of water, as discussed below.

2.2.1.1 Tension samplers

Sampling period depended on the type of porous boundary, the amount of suction, and soil characteristics. A 30-minute sampling period allowed for the collection of 5-10 mL of porewater from lacustrine and estuarine sediments with suction supplied by a 20 mL vacuum test tube (Shotbolt, 2010). A standard Rhizon sampler was advertised as being capable of sampling at 4 mL/minute (http://www.rhizosphere.com/rhizons). The actual sampling rate was also limited by the hydraulic conductivity of the sediments.

The pressure, which induces the suction, decreased as the amount of sample in storage increased (Harvey, 1993). The decreased pressure resulted in a sample primarily composed of water removed from the largest pores (Harvey, 1993). However, the proportion of water extracted from a given pore size cannot be calculated because the pressure changed continuously with an unknown magnitude. Determining the sample origin was further complicated by the unlimited volume of affected soil (Harvey, 1993). The sampling bias has the potential to create issues when attempting to interpret variations in the sampled porewater (Harvey, 1993).

Tension samplers alter porewater chemistry by disrupting the system's equilibrium. Pressure changes can alter the concentrations of various ions in the porewater (Sacchi et al., 2001). The most notable of these changes relate to carbon dioxide degassing (Sacchi et al., 2001). Further chemical changes relate to the alteration of relative amounts of sediment, water, and solutes (Sacchi et al., 2001). As water is removed from the system, solute concentrations change by ion exchange and salt precipitation (Sacchi et al., 2001). Studies quantifying these changes have largely focused on destructive sampling methods (Sacchi et al., 2001). The changes, particularly

those resulting from salt precipitation, are unpredictable (Sacchi et al., 2001). The chemical reactions that occur when using a tension sampler prevent direct sampling of porewater at equilibrium with the sediments (Sacchi et al., 2001).

2.2.1.2 Passive diffusion samplers

Passive diffusion samplers consist of a vial filled with distilled water and covered with a permeable membrane. Once deployed, the samplers typically equilibrated between one day and one month (ITRC, 2006). Equilibration time depended on the type of permeable membrane, orientation of the sampler, ambient temperature, groundwater velocity, and the analyte of interest (ITRC, 2006; Kot-Wasik et al., 2007).

Passive diffusion samplers do not exert a pressure on the porewater. Without an induced pressure gradient, the sample originated from the area immediately surrounding the sampler. The samples can be difficult to generalize to a heterogeneous system because of their small-scale collection area (Seethapathy, et al. 2008). While the spatial origin of the sample was easily identified, the temporal origin was more complicated.

A completely equilibrated sample is a time-weighted average of the local porewater (Kot-Wasik et al., 2007). The degree of weighting depended on diffusion rates specific to the analyte and the sampler design (ITRC, 2007). The sampler was not sensitive to short term variations in the system (Kot-Wasik et al., 2007). Instead, the collected sample was an average of local water composition during the deployment time weighted toward the end of the sampling period (Roll and Halden, 2016).

2.2.2 Numerical model setup

Transport of salts through the surficial sediments of the salt marsh was simulated with a numerical model distributed by USGS. The model, SUTRA, simulates density-

dependent groundwater flow and solute transport (Voss and Provost, 2002). Modifications to the model account for changes in the system's total stress caused by tidal fluctuations (Reeves et al., 2000; Wilson and Gardner, 2006). The Gardner (1958) model was used to calculate unsaturated flow properties. To simulate field conditions, the boundary conditions were based on the water salinity and meteorological data collected at nearby NERRS and CO-OPS sampling sites.

The model simulated one-dimensional vertical groundwater flow and solute transport in the top meter of marsh sediment. The sediments consisted of two layers which only differ in their porosity. The upper layer extended from the surface to 20 cm depth. This layer has an increased porosity to represent the extensive bioturbation, e.g. crab burrows, present near the marsh surface. Bioturbation decreased in the lower layer, so the porosity was reduced. The sediment characteristics of the layers were otherwise identical.

The bottom boundary separated the low permeability mud from a sandy aquifer. This boundary only responded to tidal stage. The tidal stage was important because it controls the largest changes to hydraulic head in the aquifer. When the site was flooded, the hydraulic head throughout the sediment column equaled the water level, stopping flow. The falling tide lowered the hydraulic head throughout the marsh. The head changed faster in the aquifer than the mud, inducing a downward hydraulic gradient. The gradient induced by site exposure allowed water to drain into the aquifer.

The upper boundary was set at the marsh surface. During inundation, the pressure was specified, where pressure was set according to the hydrostatic pressure from the tide. Upon exposure, the upper boundary changed to a specified flux boundary. The flux

reflected meteorological conditions. During precipitation events, the flux equaled either the rate of precipitation or the maximum rate of infiltration. The maximum rate of infiltration was defined as the flux required to fully saturate and maintain saturation in the upper sediments. The maximum rate of infiltration was used to prevent over-saturation. When water did not infiltrate from precipitation or flood water, the flux of water at the upper boundary depended on ET. ET was imposed throughout the root zone, defined as the top 25 cm of the sediment. The amount of ET decreased exponentially with depth to reflect the decreasing quantity of roots.

Unlike precipitation and water level, ET must be estimated using indirect measures. Two estimation methods were tested in this study. The Turc equation used air temperature and solar radiation to estimate monthly or daily ET (Turc, 1961). Morris (1995) used two years of ET measurements from North Inlet, South Carolina to create a sinusoidal equation relating ET to the day of the year and hour of the day. The two methods were compared in a sensitivity analysis.

The crab burrows in the upper portion of the marsh suggests the presence of multiple flow-regimes, as show in Xin (2009). Transport in two flow-regimes are frequently described with dual porosity models. These models represent the flow-regimes as two overlapping and interacting domains (Samardzioska and Popov, 2005). Dual porosity models are most useful when the two domains are densely and regularly spaced (Samardzioska and Popov, 2005). A dual porosity model could be applied to describe the bioturbated layers in detail. However, it was not used because other studies, notably Wang et al. (2007) and Hemond and Fifield (1982), successfully modeled this layer with the simpler equivalent continuum approach.

Table 2.2 lists the parameters used in the numerical model. The values used for sensitivity analyses are also listed when applicable.

2.2.3 Model calibration

Model calibrations referenced salinity data collected at Goat Island with the passive diffusion samplers (Morris, 2013) and the salinity data collected for this study using tension samplers. The simulated salinity was related to the passive diffusion sampler measurements using a time-weighted average of the simulation results. By assuming a linear weighting, the average, $\bar{c}$, is

$$\bar{c} = \sum_{i=1}^{n} {}^{1}/_{n^2} (2i - 1)c_i,$$

where n is the number of simulated salinities, c_i, during the sampling period. The tension samplers removed porewater from the entire porous portion of the sampler. Salinity from the model was adjusted to reflect the range of the sample by averaging over 10 cm depth. Calibrations included adjusting permeability, sediment compressibility, dispersivity, flow velocity, and capillary rise.

The model was also tested for delayed responses to salinity changes. A delayed response may indicate that the model estimated salinity in a slower flow regime than the observations. These temporal calibrations were achieved by adjusting the timing of the final simulated salinities. The adjustments change the absolute date associated with each data point without altering their relative dates. Adjustments between 1 and 30 days were tested.

Table 2.1 Parameters for Analytical Model

Site	*Depth (cm)*	z_0 *(cm)*	C_0 *(g/L)*	D_I *(cm)*	D_{II} *(cm)*	*u (cm/d)*
TS1	50	5	848	1.05	500	8.79
	75	5	848	0.60	800	7.75
TS2	50	0	848	3.0	7e5	8.0
	75	0	848	10	2e6	12
	75	0	848	22	2.5e6	9.0

Table 2.2 Parameters for numerical model

Parameter	*Value*	*Sensitivity Analysis*
permeability (m^2)	4e-13	4e-11 – 4e-15
Inverse capillary rise (kPa^{-1})	6.73e-05	7e-4 – 7e-6
residual saturation	0.1	
sediment compressibility (Pa^{-1})	1e-06	1e-5 – 1e-8
porosity	0.7, 0.8	
longitudinal dispersivity (cm)	3.5	0.35 – 65
drainage velocity (cm/d)	8	2 – 12
root zone depth (cm)	20	10 – 30

CHAPTER 3 RESULTS

3.1 Dye tracer study

Injecting fluorescein into a crab burrow resulted in subsurface concentrations an order of magnitude lower than those when fluorescein was injected in the shallow subsurface (Table 3.1). However, the pattern of transport remained the same. At a given observation point below the injection location, concentrations initially increased before slowly decreasing.

3.1.1 Analytical model

The analytical model and observed data were well correlated ($r^2 > 0.85$; Table 3.2). The results from the analytical model suggested a fairly constant flow velocity of 8 cm/d. Alterations to the velocity change when the peak concentration occurs and the residence time of the solute (Fig. 3.1). Three of the four modeled locations had flow velocities of 8 ± 1 cm/d. The last location, 75 cm at TS2, required a much higher velocity and dispersivity to account for all of the observed concentrations (Table 2.1). However, simulating a velocity of 9 cm/d only slightly affected the agreement between the model and the concentrations observed at 75 cm at TS2 (Table 3.2).

3.2 Salinity

3.2.1 Tension samplers

Salinities from tension samplers generally increased during the observation period, February and March 2017 (Fig. 3.2), particularly at the 10 and 25 cm observation depths. The salinity in replicate samples varied within an average range of 2.6 g/kg. The

maximum temporal variation occurred in the 10 cm samples from 27.9 g/kg February 11, 2017 to 39.9 g/kg on March 21, 2017. Salinity did not appreciably change at or below 50 cm depth.

Visual comparison of salinity with other environmental parameters (Fig. 3.3) suggested possible correlation between porewater salinity, surface water salinity and ET. Statistical analyses revealed the porewater salinity correlated only with surface salinity and air temperature (Table 3.3). Surface salinity was positively correlated with salinities at 10 cm and 25 cm. Air temperature was positively correlated with salinity, a proxy for ET, at 10 cm, 50 cm, and 75 cm. Porewater salinity had no significant correlation with hydroperiod. However, sample size was small and further studies may illuminate other relationships.

3.2.2 Passive diffusion samplers

The salinity obtained from the passive diffusion samplers between January 2016 and March 2017 shows generally higher salinities in the summer than the winter (Fig. 3.4A). Porewater salinity from passive diffusion samples had a weak, but significant, correlation with precipitation at 75 cm and 100 cm (Table 3.4). This relationship was evident in the maximum and minimum salinities measured throughout the 23.4 years passive diffusion samplers have been in use at Goat Island. The lowest salinity, 5.8 g/kg, occurred in May 2015 at a depth of 75 cm. Less than a week before the sample was collected, tropical storm Ana made landfall near North Inlet. The NERRS station at Oyster Island recorded more than 10 cm of rain over the next four days. The salinity reached a maximum of 49.4 g/kg in August 1999 at 10 cm depth during a drought (South

Carolina State Climatology Office, 1999). The salinity from the passive diffusion samplers did not correlate with hydroperiod, surface salinity, or ET.

3.2.3 Numerical model

The numerical model produced salinities that did not correlate with hydroperiod, surface salinity, precipitation, or ET (Table 3.5). In simulations, the variability of porewater salinity decreased with depth, consistent with field observations from the tension samplers. Increased depth also resulted in local maximum and minimum salinities occurring later (Fig. 3.5).

During February and March 2017, the simulated porewater was generally more saline than the passive diffusion samples and less saline than the tension sampler values (Fig. 3.6). Results from the simulations and the two observation methods all showed that salinity became more constant with depth. The simulated salinities and the salinities from the tension samplers were more variable at the shallower observation points, but the variations appear unrelated. For example, in mid-February salinities from the tension samplers increased while simulated salinities quickly decreased. For the same period, the salinity from the passive diffusion samplers did not change.

The simulated salinities did not correlate with either the tension sampler salinities or the passive diffusion sampler salinities (Table 3.6). The model's best, though insignificant, correlation ($r^2 = 0.23$) was with the tension samplers 50 cm below the marsh surface. The root mean square error did not change when comparing the model to different sampling methods. However, the model agreed well with the salinity of the passive diffusion samples from March and April 2017 (Fig. 3.7). The model values most closely agreed with the passive diffusion samplers at 100 cm. The result was a root

mean squared error of 8.5 g/kg, which is 1.6 times less than the largest variation in results from replicate samplers. Correlation and error improved with depth regardless of the sampling method.

Agreement between the model and the tension sampler salinities increased with a temporal shift (Table 3.6). At 10 cm, 25 cm, and 75 cm depth, the correlation coefficient increased by an order of magnitude or more if the model was assumed to lag the observed salinities by 4-21 days. The delay also slightly decreased the error. The length of delay needed to provide maximum correlation decreased sharply between 10 cm and 25 cm.

Adding a delay did not improve agreement between the passive diffusion sampler salinities and the model (Table 3.6).

3.3 Porewater salinity model sensitivity analysis

The model was tested for sensitivity to surface salinity, groundwater flow velocity, dispersivity, sediment compressibility, permeability, capillary rise, and meteorological conditions. Sensitivity analyses (Fig. 3.8) were performed to gauge the impact of different conditions on the simulated soil salinity.

Surface water salinity impacted the magnitude of porewater salinity more than any other tested variable. Any change in surface salinity caused a proportional change to the porewater salinity. While surface salinity altered the absolute value of the porewater salinity, its impact on the direction and relative magnitude of the change was small.

The velocity of drainage altered the dominant source of porewater. High velocities drained the system and allowed for greater surface water infiltration. The salinity then reflected the salinity of the surface water more closely. Concentrations of solutes in porewater from low velocity systems responded more slowly to surficial

changes. Fewer tidal inundations and increased ET appeared to exacerbate the salinity differences between simulations using high and low velocities.

Alterations to the dispersivity affected the degree to which salinity changed over short time periods. Increased dispersion intensified mixing, which resulted in decreased sensitivity to rapid environmental changes. Systems with small dispersivities experienced a larger variety of salinities than systems with larger dispersivities.

Soil compressibility and capillary rise altered the porewater salinity calculated by the model. The changes that resulted from altering the compressibility or capillary rise did not have a clear pattern and likely do not represent real processes. When altering compressibility, the model may use the proportionality between saturation and hydraulic conductivity to increase infiltration velocity. Compressible sediments were able to release more water from storage without allowing air into the system than less compressible sediments. The presence of air in the sediments reduced hydraulic conductivity. Lower hydraulic conductivity at the surface decreased the rate of infiltration. Less infiltration subdued the response of porewater to environmental responses.

Increased permeability increased the average salinity of the system at 10 cm. Low permeability sediments retained fresh water resulting from rain or flooding longer than sediments with higher permeability. The longer retention time also resulted in a system with less sensitivity to short term variations in meteorological and water quality conditions.

The average hydroperiod changed porewater salinity by altering the importance of other variables. When the average hydroperiod was large, porewater salinity began to

behave more like surface salinity. Frequent flooding also increased the range of salinity at 10 cm depth. As the hydroperiod decreased, the porewater salinity became more sensitive to short term variations, such as changing weather.

Meteorological conditions did not significantly impact the simulated porewater salinity. Porewater salinity was insensitive to the timing and amount of precipitation. The model was also insensitive to the depth of the root zone, which defines where ET occurs. The method of calculating ET did not change the simulated salinity. However, porewater salinity was slightly sensitive to the amount of ET. Porewater salinity responded to changes in ET during periods of infrequent flooding. Precipitation and ET moved far less water through the system than the tidal cycle. Changes due to variations in surface water salinity largely obscured changes from the weather.

Table 3.1 Fluorescein concentration

Site	*Day*	*10*	*25*	*50*	*75*
TS1	3	60 ± 30	9.5 ± 0.3	10 ± 10	1.1 ± 0.4
	7	50 ± 40	11 ± 1	11 ± 6	1 ± 6
	10	60*	10.63 ± 0.07	3 ± 5	20 ± 10
	14	20*	10.2 ± 0.6	0.5 ± 0.1	0.3 ± 0.3
	18	10 ± 1	11*	1 ± 3	0.061 ± 0.006
	24	9*	18*	—	—
TS2	3	0.05*	6*	0.4 ± 0.3	0.3 ± 0.6
	7	0.0 ± 0.1	1 ± 2	0.5 ± 0.3	0.11 ± 0.04
	10	0.2 ± 0.3	2.5 ± 0.6	0.31 ± 0.04	0.14 ± 0.07
	14	0.2 ± 0.3	1 ± 2	0.1 ± 0.2	0.054 ± 0.003
	18	0.2 ± 0.4	1 ± 1	0.11 ± 0.05	0.059 ± 0.004
	24	0.2 ± 0.4	1 ± 2	—	—

*No replicate samples available

Table 3.2 Dye tracer study: Comparison between simulated and observed concentrations

Site	*Depth (cm)*	r^2	*p*	*RMSE*
TS1	50	0.873	0.02	2.88
	75	0.999	7e-6	0.49
TS2	50	0.982	0.001	0.08
	75	0.982	0.001	0.03
	75	0.946	0.005	0.01

Table 3.3 Correlation of tension sampler salinity with meteorological and water quality data*

	Hydroperiod		*Surface Salinity*		*ET*	
Depth (cm)	r^2	p	r^2	p	r^2	p
10	1e-4	0.9	**0.54**	0.04	**0.68**	0.01
25	0.009	0.8	**0.65**	0.02	0.37	0.1
50	0.19	0.4	0.32	0.2	**0.91**	0.003
75	0.04	0.7	0.13	0.5	**0.79**	0.02

* Pearson correlation test with significance level $\alpha = 0.05$, bold typeface indicates significant correlation

Table 3.4 Correlation of passive diffusion sampler salinity with meteorological and water quality data*

	Hydroperiod		*Surface Salinity*		*Precipitation*		*ET*	
Depth (cm)	r^2	p	r^2	p	r^2	p	r^2	p
10	0.03	0.5	0.14	0.2	0.004	0.8	0.2	0.09
25	0.15	0.1	0.11	0.2	0.02	0.6	0.09	0.3
50	0.06	0.4	0.18	0.1	0.23	0.07	0.05	0.4
75	0.04	0.5	0.18	0.1	**0.28**	0.04	0.03	0.5
100	0.07	0.3	0.18	0.1	**0.31**	0.03	0.04	0.5

* Pearson correlation test with significance level $\alpha = 0.05$, bold typeface indicates significant correlation

Table 3.5 Correlation of simulated salinity with meteorological and water quality data*

	Hydroperiod		*Surface Salinity*		*Precipitation*		*ET*	
Depth (cm)	r^2	p	r^2	p	r^2	p	r^2	p
10	**0.08**	5e-08	**0.05**	1e-05	0.01	0.09	**0.03**	0.002
25	**0.05**	9e-06	**0.06**	4e-06	0.01	0.1	**0.02**	0.003
50	**0.03**	0.002	**0.04**	7e-05	0.01	0.1	**0.02**	0.004
75	**0.02**	0.02	**0.02**	0.003	0.01	0.1	**0.02**	0.01
100	**0.01**	0.03	**0.02**	0.01	0.01	0.1	**0.01**	0.02

* Pearson correlation test with significance level $\alpha = 0.05$, bold typeface indicates significant correlation

Table 3.6 Correlation of simulated salinity with observed salinity*

			r^2		p		*RMSE*	
	Depth (cm)	*Delay (days)*	*Standard*	*Delayed*	*Standard*	*Delayed*	*Standard*	*Delayed*
Passive diffusion samplers	10	28	0	0.01	0.99	0.72	14.2	14.3
	25	8	0.07	0.07	0.35	0.35	12.4	12.4
	50	8	0.17	0.17	0.15	0.15	10.7	10.7
	75	8	0.13	0.13	0.2	0.2	9.8	9.8
	100	0	0.19	0.19	0.12	0.12	8.4	8.4
Tension samplers	10	21	0.03	**0.78**	0.68	0	13.8	8.1
	25	5	0.002	**0.72**	0.92	0.01	10.4	9.5
	50	3	0.23	0.46	0.33	0.14	10.3	9.7
	75	4	0.08	**0.8**	0.6	0.02	9.7	9.5

*Pearson correlation test with significance level $\alpha = 0.05$, n = 8, bold typeface indicates significant correlation

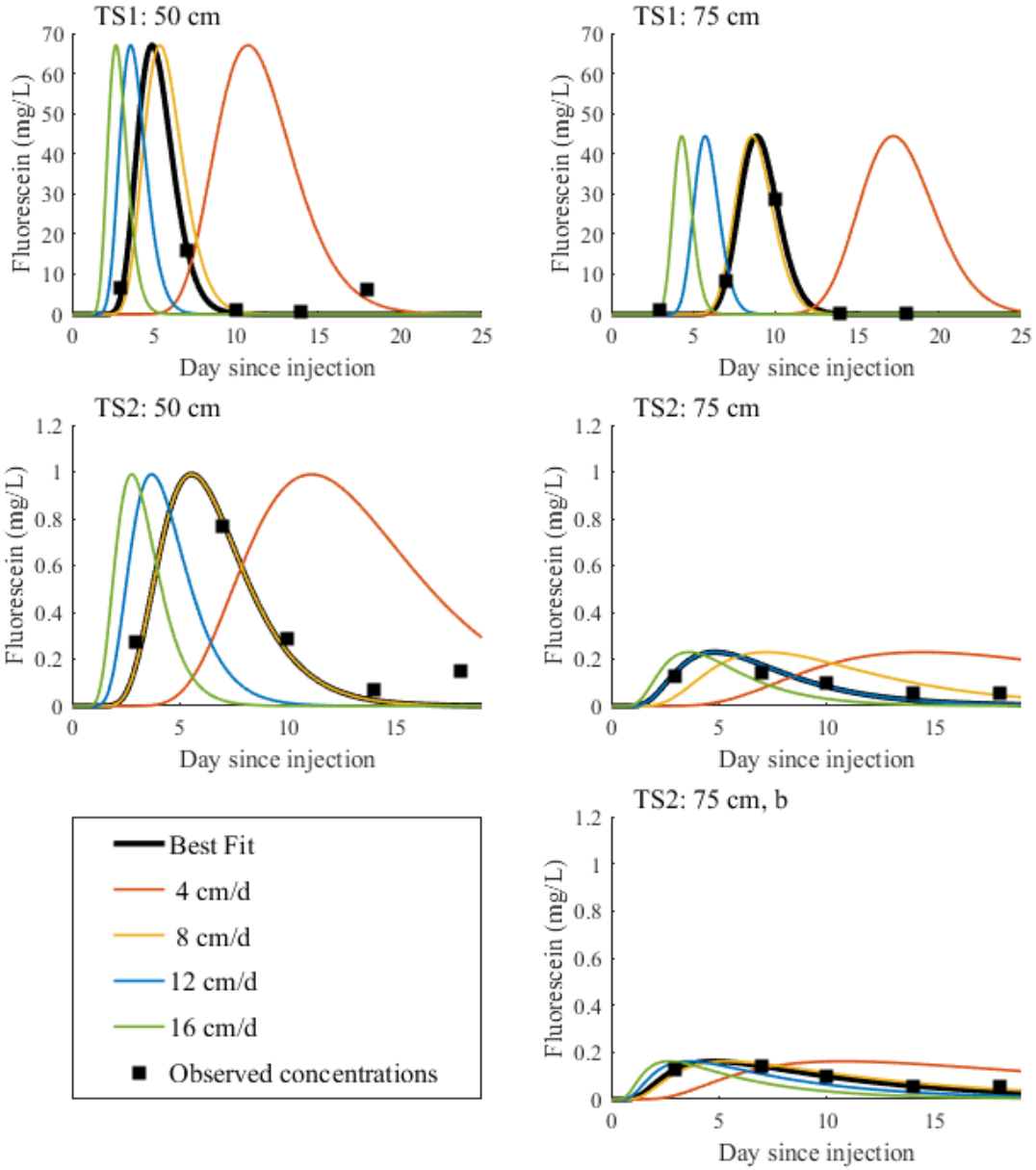

Figure 3.1 The analytical model of fluorescein concentrations. The tracer was injected on day 0. The black squares mark the observed concentrations. The black line indicates the best fit solution, which used the parameters listed in Table 1. The other lines show solutions with various velocities between 4 cm/d and 16 cm/d to provide context for the velocity calculated using the best fit solution.

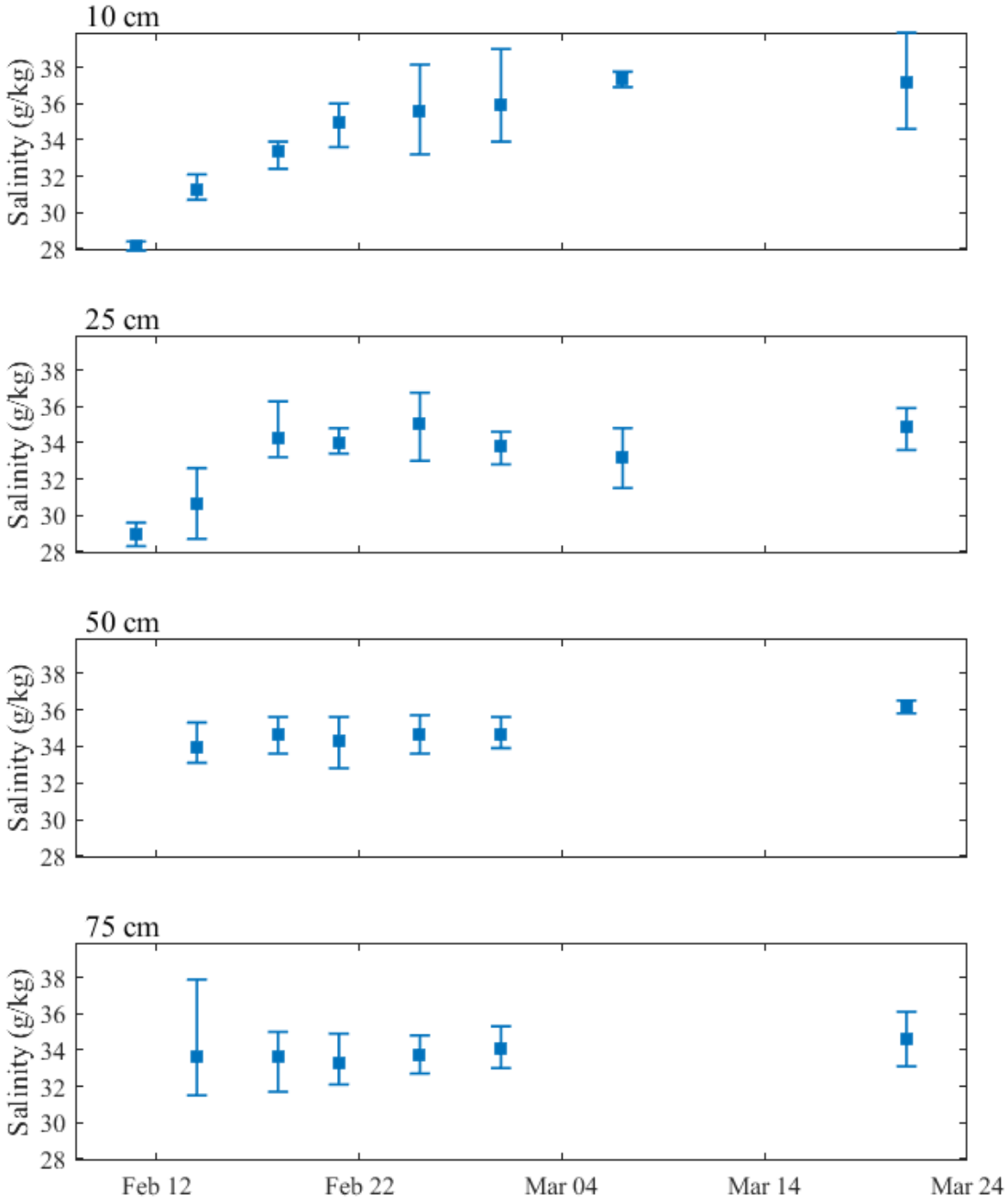

Figure 3.2 Salinity data collected using tension samplers at Goat Island. The squares mark the geometric mean of all of the samples on a given day. The bars indicate the range of sample salinities.

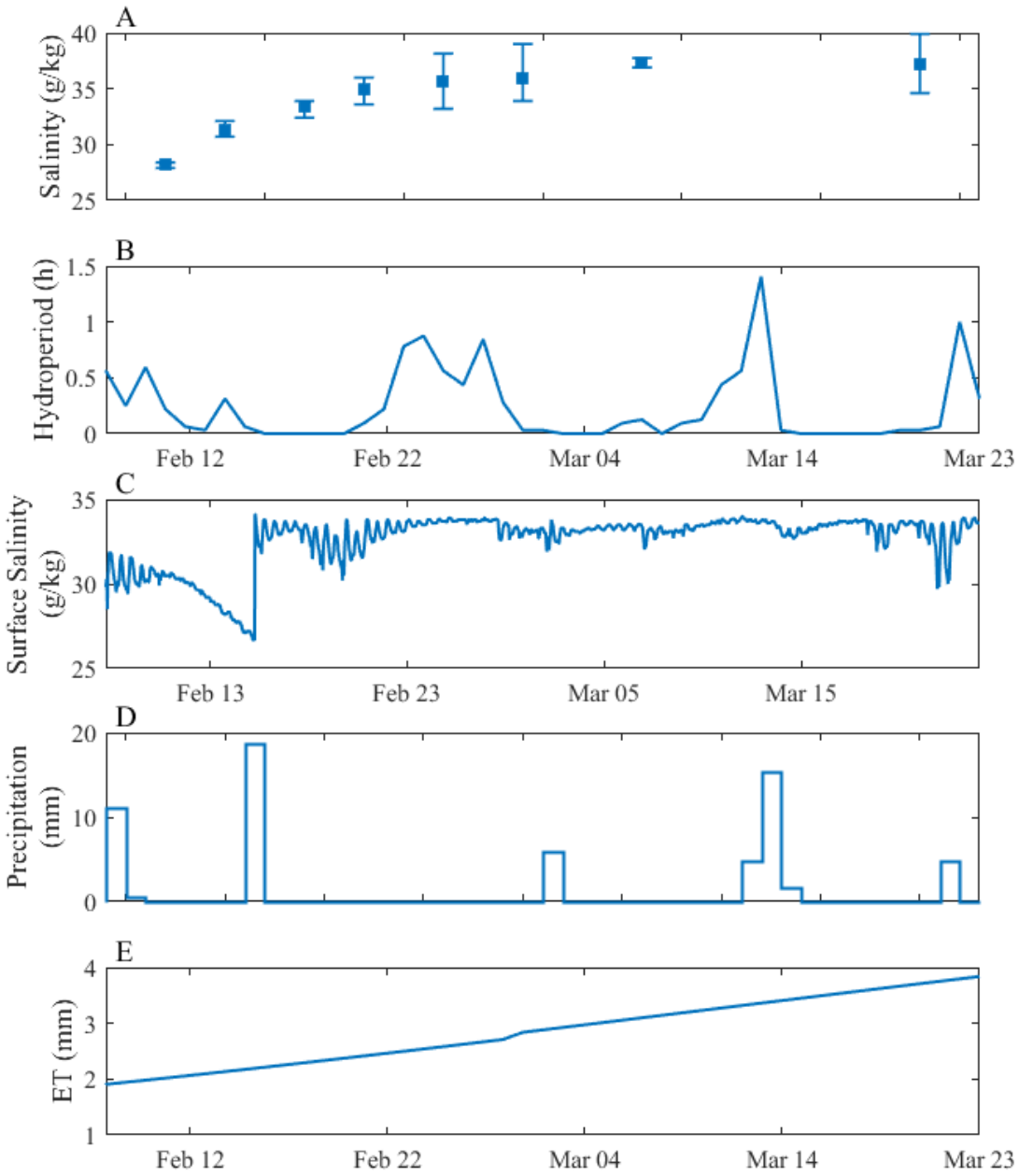

Figure 3.3 Salinity of samples taken from the tension samplers at 10 cm compared with the surficial conditions of the sampling period. (A) The geometric mean of the salinity samples at 10 cm depth (blue square) with the range indicated by the bars. (B) The depth of water relative to the site, such that when depth is less than zero the site is exposed. (C) The salinity of the creek water. (D) The amount of rain on a given day. (E) The amount of ET occurring on a day, calculated using the equation presented by Morris (1995).

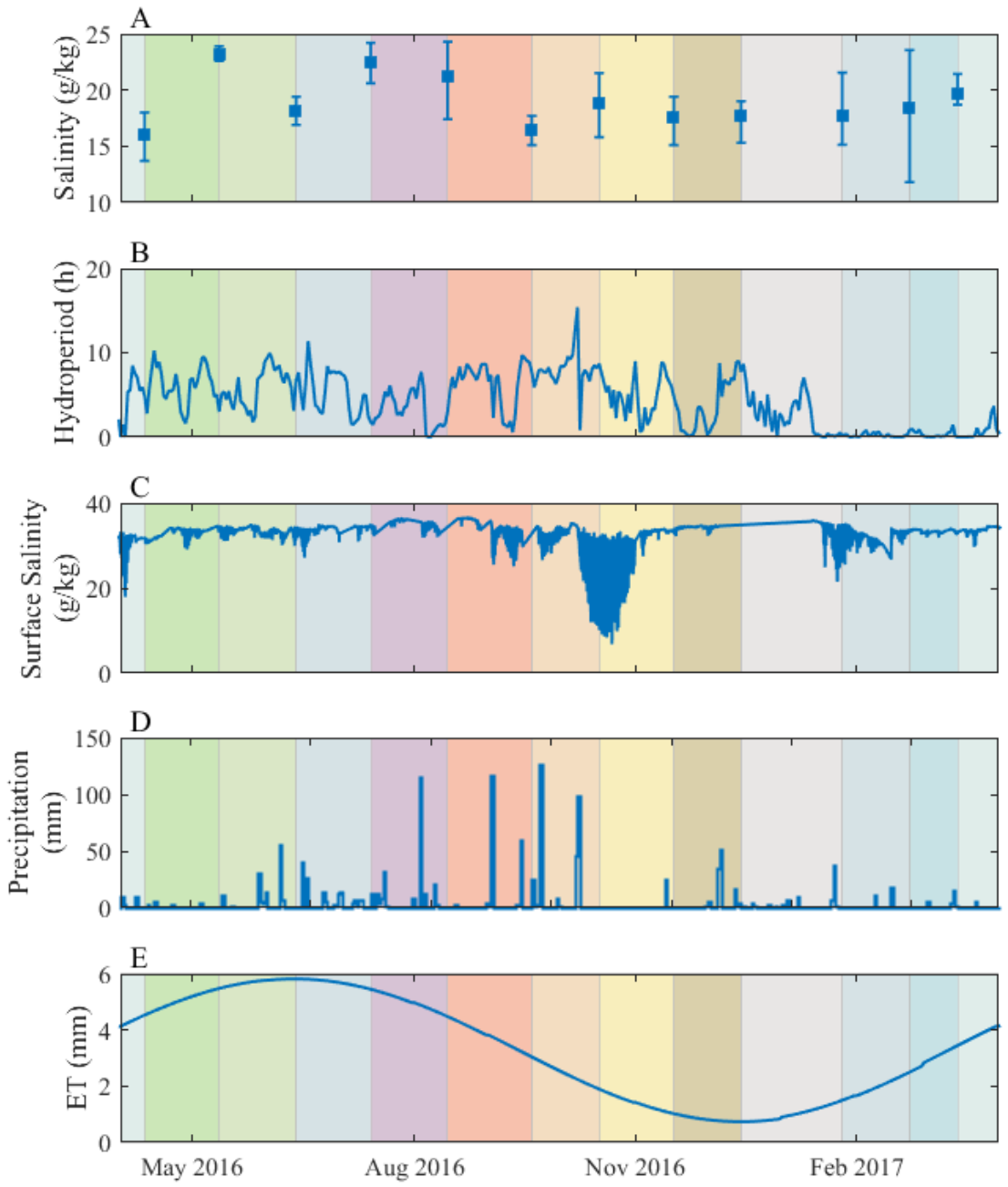

Figure 3.4 One year of salinity data from PDS at 10 cm with surficial conditions. The colored bands mark the period of sample deployment. As PDS provide a time-integrated concentration, the conditions throughout the preceding band impact the concentration reported by the sampler. (A) The geometric mean of the salinity samples at 10 cm depth (blue square) with the range indicated by the bars. (B) The depth of water relative to the site, such that when depth is less than zero the site is exposed. (C) The salinity of the creek water. (D) The amount of rain on a given day. (E) The amount of ET occurring on a day, calculated using the equation presented by Morris (1995).

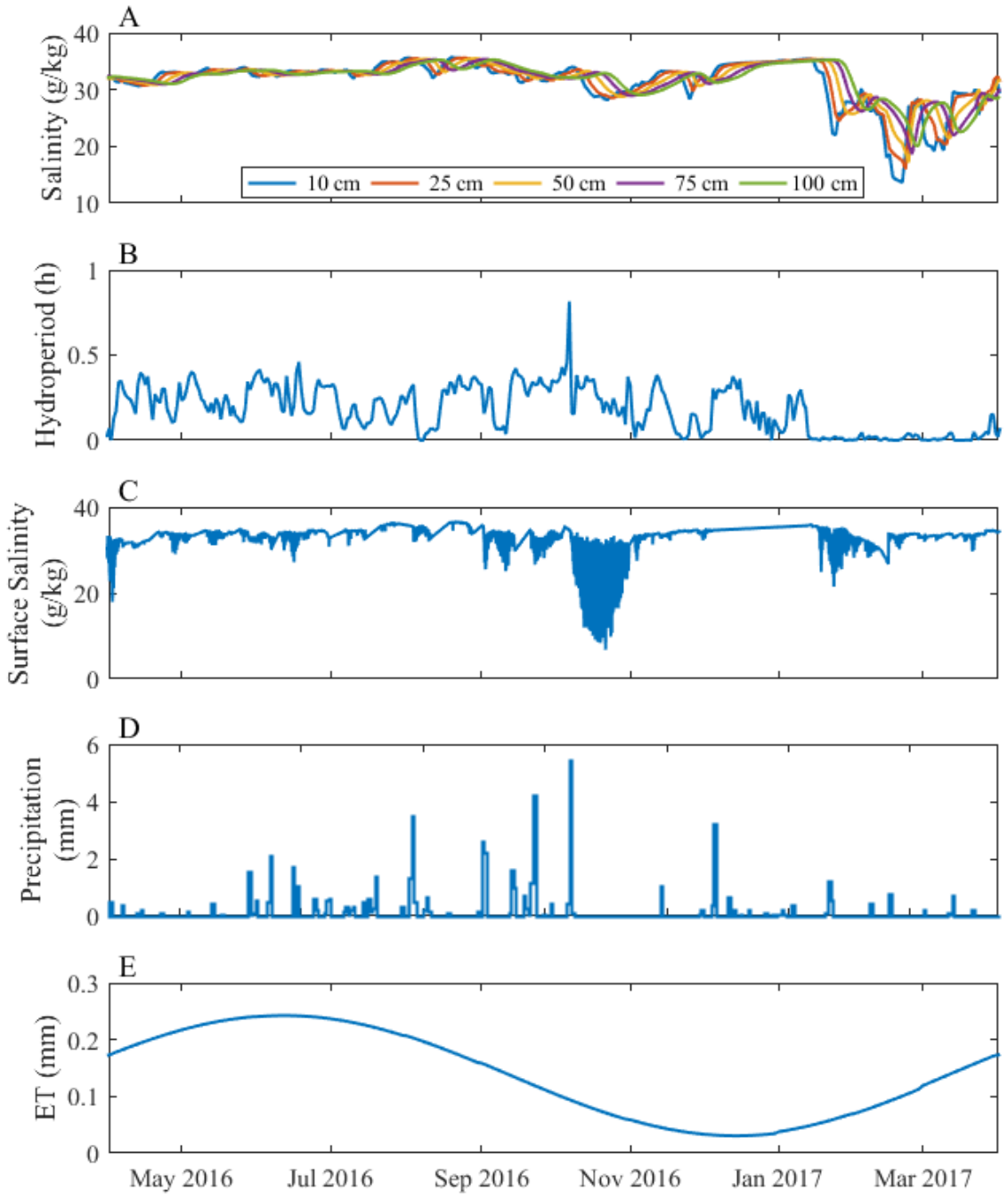

Figure 3.5 One year of simulated salinity concentrations at Goat Island. (A) The salinity at 10, 25, 50, 75, and 100 cm are plotted using different colors. (B) The depth of water relative to the site, such that when depth is less than zero the site is exposed. (C) The salinity of the creek water. (D) The amount of rain on a given day. (E) The amount of ET occurring on a day, calculated using the equation presented by Morris (1995).

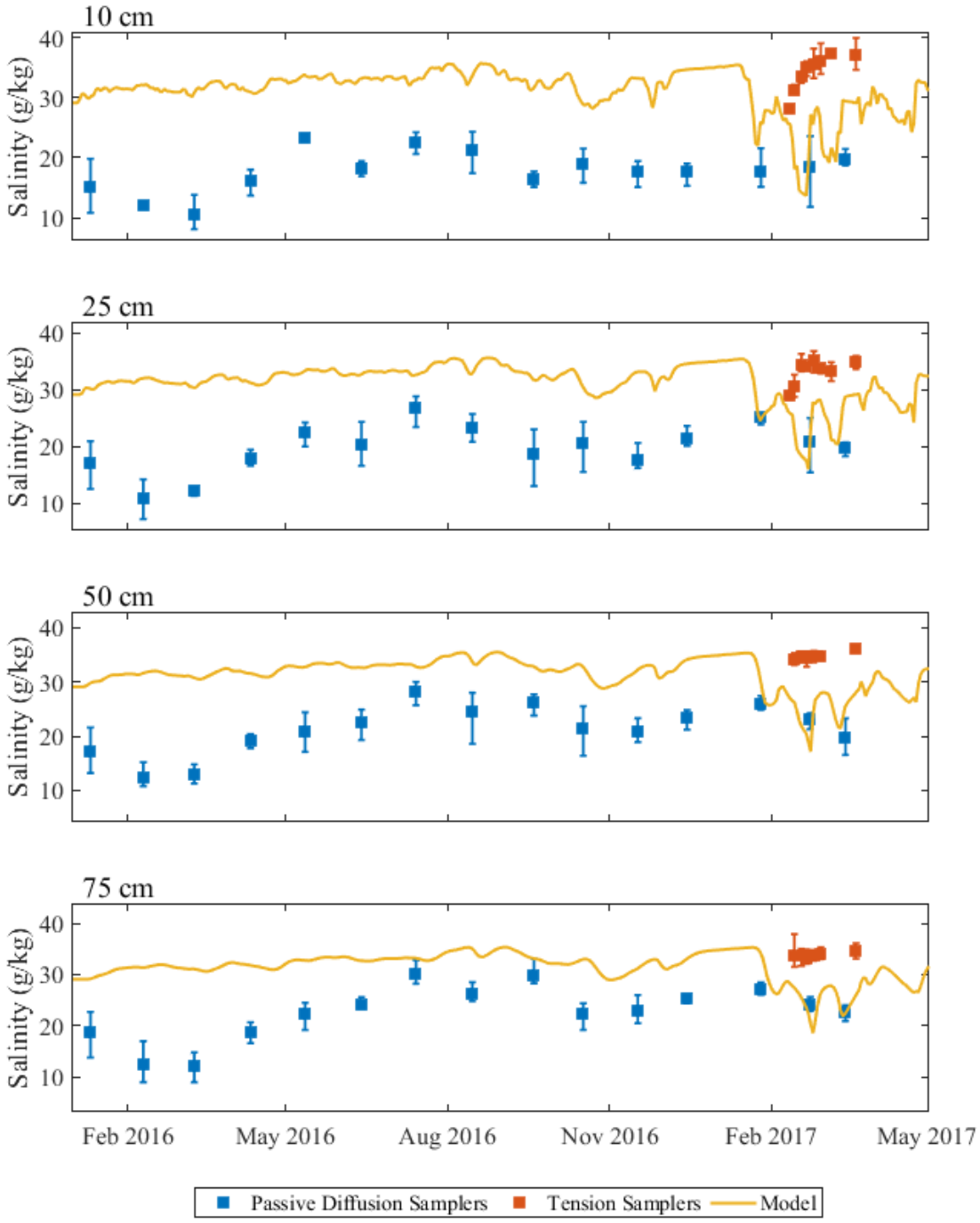

Figure 3.6 Comparison of methods. The geometric means of the replicate samples of the tension samplers (orange) and the passive diffusion samplers (blue) are indicated by squares. The range of measured salinities is indicated by the bars. The yellow line marks the salinity as calculated by the model.

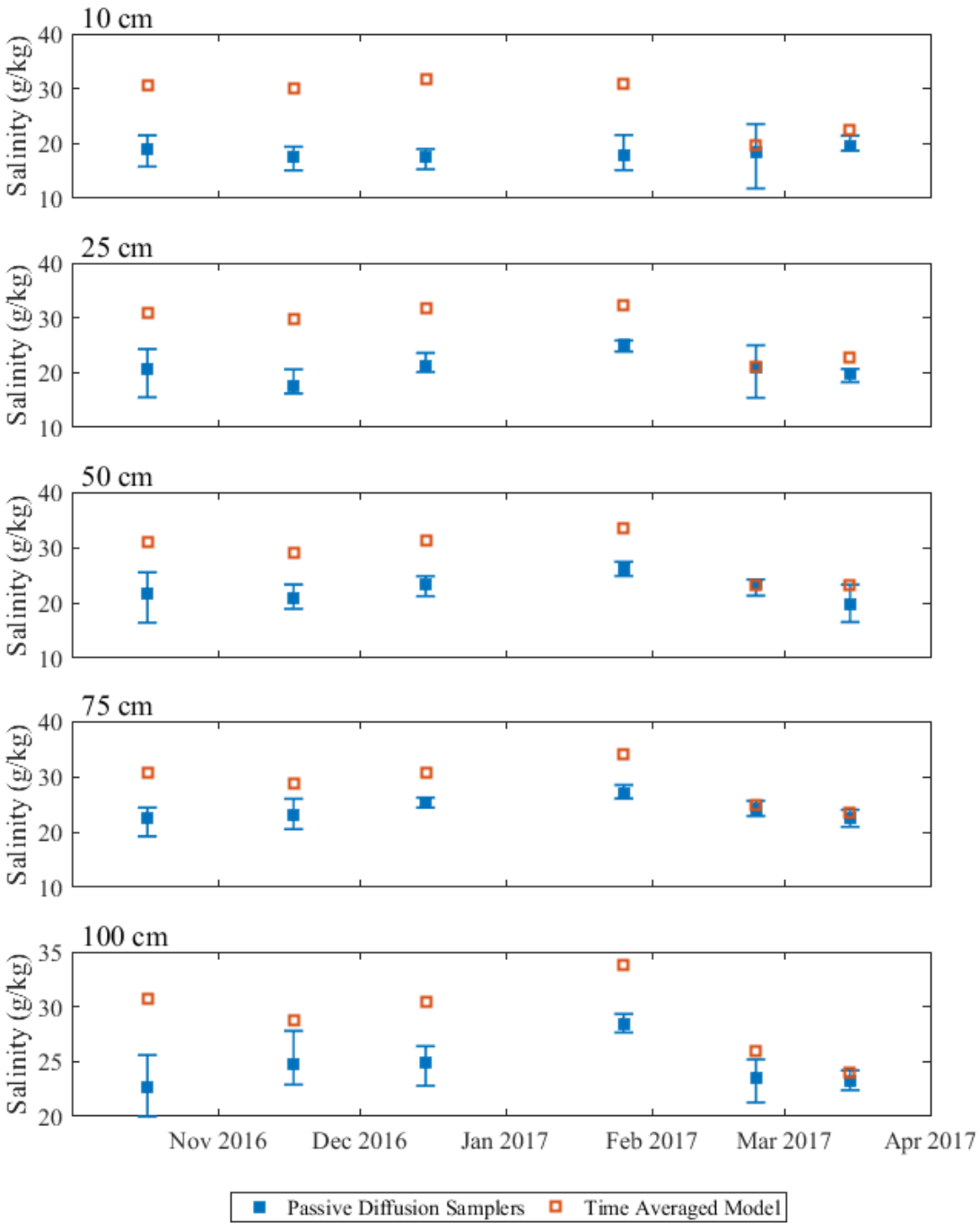

Figure 3.7 Time weighted averages from the model simulation compared to salinities measured by passive diffusion samplers

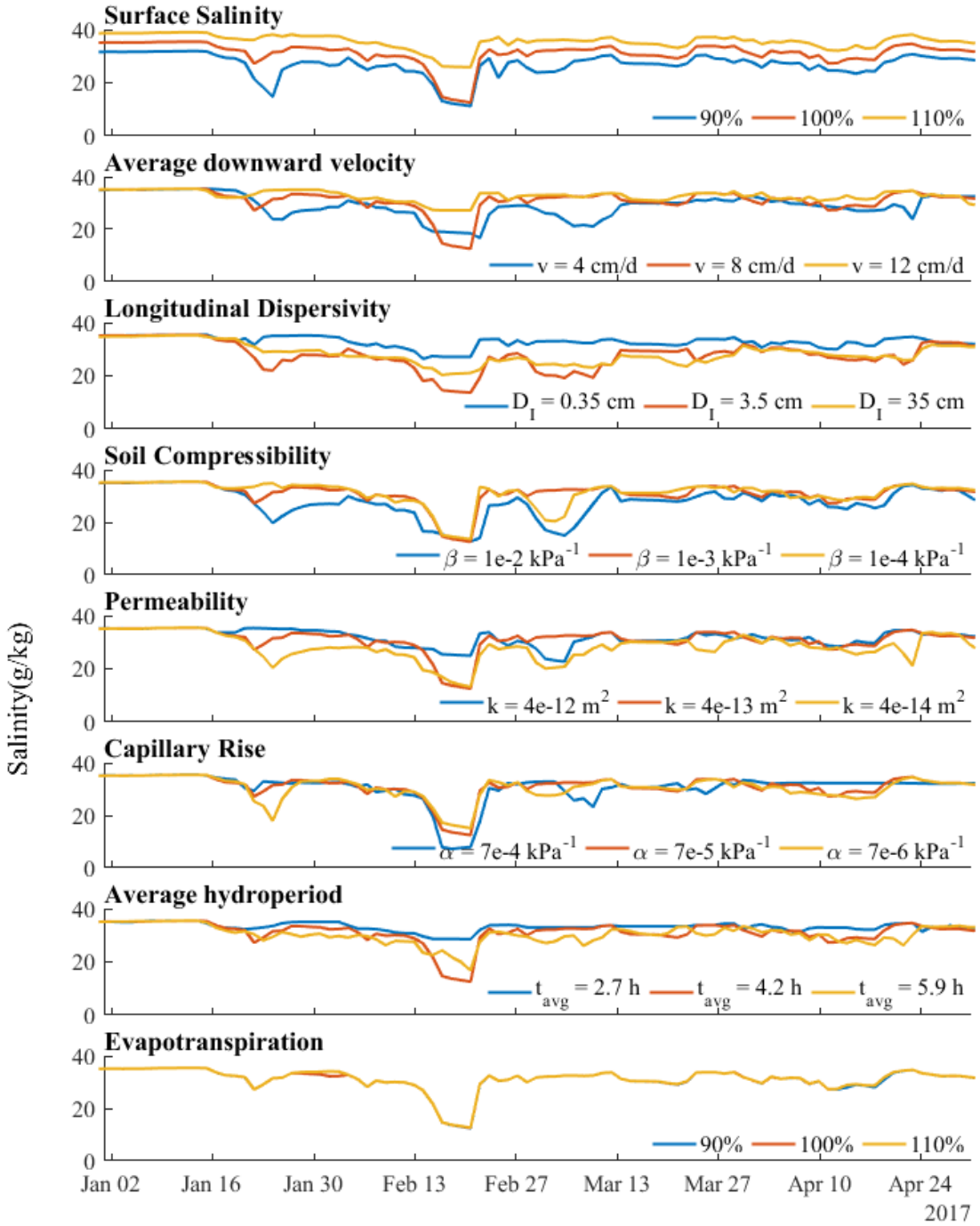

Figure 3.8 Sensitivity analysis results at 10 cm. Surface salinity and ET are identified by percent of the observed value. Average downward velocity, longitudinal dispersivity, soil compressibility, permeability, and capillary rise are described by the value assigned throughout the simulation.

CHAPTER 4 DISCUSSION

4.1 Dye tracer study

The velocity resulting from the tracer study was much larger than expected. The velocity calculated from the tracer study was 8 cm/d. Morris (1995) used 0.94 cm/d in the model of salinity in the top 30 cm of the marsh at Goat Island. The difference could be due to the greater depth of the tracer study. The sediment at Goat Island became sandier with depth, which would allow for higher velocities lower in the sediments. Also, temporal differences in velocity could cause the discrepancy. The average flow velocity during February and March may be much higher than the rest of the year. Groundwater discharge from salt marshes increases when mean water level is low (Hughes et al. 2015; Wilson et al. 2015), and mean water level is typically lowest in February and March at North Inlet.

The velocity calculated for 75 cm at TS2 was particularly high. The model indicated a velocity 1.4 times larger than the average velocity of all the modeled locations. An alternative solution for 75 cm at TS2 allowed for a lower velocity, but agreement between the solution and the observations also decreased. The difference in velocity between locations could be due to heterogeneity or measurement limitations. Preferential flow paths, such as macro-pores, could also affect the velocity. The higher velocity calculated for 75 cm at TS2 may also be due to the low fluorescein concentrations. The fluorescein concentrations measured at the site are too low to be confident that variations are not just caused by natural fluorescence.

4.2 Salinity

The salinity also exhibited a wide variability, most noticeably between sampling methods. Samples collected with tension samplers tended to be 5-10 g/kg more saline than the passive diffusion samples. Some difference was expected because the two types of samplers take inherently different measurements. Tension samplers provided point measurements. Passive diffusion samplers collected a time-weighted average biased towards current conditions (Roll and Halden, 2016). Theoretically, a time-weighted average of point measurements from tension samplers can approximate the concentrations from passive diffusion samplers. However, during February and March 2017, the maximum salinity reported by the passive diffusion samplers was 25.62 g/kg while the tension samplers' minimum salinity was 27.9 g/kg. An average cannot relate the two salinities. The relationship between the passive diffusion samplers and tension samplers used in Goat Island's high marsh was more complicated than originally expected.

The salinity differences reflect chemical changes which occurred because of the sampling. The passive diffusion sampler does not alter the porewater equilibrium. Because the equilibrium was maintained, the sample reflects the composition of the original porewater. The tension sampler, by disrupting the equilibrium, may remove a sample with constituents originating from reactive minerals and ions sorbed to the sediments (Sacchi et al., 2001).

Macro-pores may also be responsible for the difference in the simulated and observed salinities. Xin et al. (2009) showed that including crab burrows as macro-pores changes the flow, water exchange, and pore pressure in a salt marsh groundwater model.

The model implemented in this study assumed a uniform pore size and accounted for macro-pores by increasing the density of pores. The parameters defining soil properties are also more closely aligned with the matrix. Therefore, the simulated values should more closely represent the matrix than the salinity of the macro-pores.

Changes take longer to propagate into the matrix than the macro-pores, so the model should lag behind the measurements from the tension samplers. The temporal difference depended on the degree of contrast between hydraulic conductivities (Zinn et al., 2004). The model was delayed compared to the tension samplers. However, the model did not have a clear delay when compared to the passive diffusion samplers. The lack of delay compared to the passive diffusion samples suggested that the samplers were sourced primarily from the matrix, because the model simulates salinity primarily from the macro-pores.

The delay calculated for the tension samplers generally decreased with depth, indicating a decreasing difference in the hydraulic conductivity of the matrix and macro-pores. Between 10 cm and 25 cm, the delay decreased by 80%. Bioturbation, such as crab burrows, also decreased sharply below 20 cm. Without the macro-pores formed from the crab burrows, the sediments have an essentially uniform hydraulic conductivity. The length of delays only decreased slightly between 25 cm and 100 cm. This smaller change may be related to the increasing particle size observed by Bradley and Morris (1990). Changes in the lag time indicate that macro-pores have a temporal effect on flow, again altering sampling source.

CHAPTER 5 CONCLUSION

Three methods were used to calculate salinity, and each produced a different result. The porewater removed by tension samplers was consistently more saline than the porewater measured by the passive diffusion samplers. The simulated salinity values fell between the two.

The salinity from the tension samplers was 5-10 g/kg more saline than the salinities from the passive diffusion samplers. This difference relates to the porewater population sampled by the two methods. The tension samplers used a low suction to withdraw porewater. The low suction could only remove water from macro-pores. Passive diffusion samplers did not rely on suction, which allowed the sample to more closely resemble the matrix porewater.

The process-based numerical model simulated salinity in the top meter of sediments. The model was most sensitive to the salinity of the flood water. The model also showed a strong response to the average downward flow velocity. This velocity was constrained using a tracer study, which indicated an average flow velocity of about 8 cm/d. The model also showed sensitivity to dispersivity, sediment compressibility, and permeability. The model was only slightly sensitive to weather conditions, such as the amount of ET or precipitation. The model used field observations to simulate the porewater salinity. However, the results did not agree with salinities from either porewater sampling method.

The likely cause of disagreement between the three methods was preferential flow, specifically, preferential flow associated with crab burrows and decayed roots. The samplers interacted with different flow regimes and the model simulated a combination of regimes. The salinity values indicated that the model may represent to some extent the salinity of both macro-pores and matrix. Identifying the level of agreement with either regime was complicated by the different temporal coverage of the samples and the model's lack of differentiation between flow regimes.

This study would be improved by increasing the sampling period and implementing a dual porosity model.

REFERENCES

Ansede, J. H., P. J. Pellechia, and D. C. Yoch. 1999. Selenium biotransformation by the salt marsh cordgrass Spartina alterniflora: Evidence for dimethylselenoniopropionate formation. Environmental Science and Technology 33:2064–2069.

Bear, J. 1961. Some experiments in dispersion. Journal of Geophysical Research 66:2455–2467.

Bradley, P. M., and J. T. Morris. 1990. Physical characteristics of salt marsh sediments: ecological implications. Marine Ecology Progress Series 61:245–252.

Catallo, W. J., and T. Junk. 2003. Effects of static vs. tidal hydrology on pollutant transformation in wetland sediments. Journal of environmental quality 32:2421–2427.

De Josselin De Jong, G. 1958. Longitudinal and transverse diffusion in granular deposits. Eos, Transactions American Geophysical Union 39:67–74.

Gardner, L. R., and B. Kjerfve. 2006. Tidal fluxes of nutrients and suspended sediments at the North Inlet-Winyah Bay National Estuarine Research Reserve. Estuarine, Coastal and Shelf Science 70:682–692.

Gardner, L. R., and H. W. Reeves. 2002. Spatial patterns in soil water fluxes along a forest-marsh transect in the southeastern United States. Aquatic Sciences 64:141–155.

Gardner, L. R., and D. E. Porter. 2001. Stratigraphy and geologic history of a southeastern salt marsh basin North Inlet, South Carolina, USA. Wetlands Ecology and Management 9:371–385.

Gardner, W. R. 1958. Some stead-state solutions of the unsaturated moisture flow equation with application to evaporation from a water table. Soil Science 85:228–232.

Harvey, J. W. 1993. Measurement of variation in soil solute tracer concentration across a range of effective pore sizes. Water Resources Research 29:1831–1837.

Hemond, H. F., and J. L. Fifield. 1982. Subsurface flow in salt marsh peat: A model and field study. Limnology and Oceanography 27:126–136.

Howes, B. L., J. W. H. Dacey, and D. D. Goehringer. 1986. Factors Controlling the Growth Form of Spartina Alterniflora: Feedbacks Between Above-Ground Production, Sediment Oxidation, Nitrogen and Salinity. The Journal of Ecology 74:881.

Hughes, A. L. H., A. M. Wilson, and J. T. Morris. 2012. Hydrologic variability in a salt marsh: Assessing the links between drought and acute marsh dieback. Estuarine, Coastal and Shelf Science 111:95–106.

Interstate Technology Regulatory Council. 2006. Technology Overview of passive sampler technologies:156pp.

Kot-Wasik, A., B. Zabiegała, M. Urbanowicz, E. Dominiak, A. Wasik, and J. Namieśnik. 2007. Advances in passive sampling in environmental studies. Analytica Chimica Acta 602:141–163.

Linden, D. R. 1977. Design, installation, and use of porous ceramic samplers for monitoring soil-water quality. Washington, D.C.

Litaor, M. I. 1988. Review of soil solution samplers. Water Resources Research 24:727–733.

Moore, W. S. 1999. The subterranean estuary: a reaction zone of ground water and sea water. Marine Chemistry 65:111–125.

Moore, W. S., J. Krest, G. Taylor, E. Roggenstein, S. Joye, and R. Lee. 2002. Thermal evidence of water exchange through a coastal aquifer: Implications for nutrient fluxes. Geophysical Research Letters 29:44–49.

Morris, J. T. 1995. The Mass Balance of Salt and Water in Intertidal Sediments: Results from North Inlet, South Carolina. Estuaries 18:556.

Morris, J. T., B. Haskin, R. L. Krest, W. Hankinson, K. Sundberg, and D. Rodriguez. 2013. Long-term Spartina alterniflora biomass, productivity, porewater chemistry and marsh elevation in North Inlet Estuary, Georgetown, SC: 1984-2012 [comma delimited digital data and spreadsheet]. Belle W. Baruch Institute for Marine Biology and Coastal Research, University of South Carolina, Georgetown, South Carolina.

Reeves, H. W., P. M. Thibodeau, R. Underwood, and L. R. Gardner. 2000. Incorporation of total stress changes into the ground water model SUTRA. Ground water 38:89–98.

Roll, I. B., and R. U. Halden. 2016. Critical review of factors governing data quality of integrative samplers employed in environmental water monitoring. Water Research 94:200–207.

Samardzioska, T., and V. Popov. 2005. Numerical comparison of the equivalent continuum, non-homogeneous and dual porosity models for flow and transport in fractured porous media. Advances in Water Resources 28:235–255.

Seethapathy, S., T. Górecki, and X. Li. 2008. Passive sampling in environmental analysis. Journal of Chromatography A 1184:234–253.

Shotbolt, L. 2010. Pore water sampling from lake and estuary sediments using Rhizon samplers. Journal of Paleolimnology 44:695–700.

South Carolina State Climatology Office. 1999. South Carolina Current Drought Status. http://www.dnr.sc.gov/climate/sco/Drought/Drought_press/release_Aug11_1999.php.

Turc, L. 1961. Evaluation des besoins en eau d'irrigation, évapotranspiration potentielle. Annales Agronomiques 12:13–49.

Voss, C., and A. Provost. 2002. A model for saturated-unsaturated, variable-density ground-water flow with solute or energy transport. U.S. Geological Survey water-resources investigations report 02-4231.

Wang, H., Y. P. Hsieh, M. A. Harwell, and W. Huang. 2007. Modeling soil salinity distribution along topographic gradients in tidal salt marshes in Atlantic and Gulf coastal regions. Ecological Modelling 201:429–439.

Weis, J. S., and P. Weis. 2004. Metal uptake, transport and release by wetland plants: Implications for phytoremediation and restoration. Environment International 30:685–700.

Whiting, G. J., and D. L. Childers. 1989. Subtidal advective water flux as a potentially important nutrient input to southeastern U.S.A. Saltmarsh estuaries. Estuarine, Coastal and Shelf Science 28:417–431.

Wiegert, R. G., and B. J. Freeman. 1990. Tidal salt marshes of the southeast Atlantic Coast: a community profile. U.S. Fish and Wildlife Service, Washington, D.C., USA.

Wilson, A. M., T. B. Evans, W. S. Moore, C. A. Schutte, and S. B. Joye. 2015. What time scales are important for monitoring tidally influenced submarine groundwater discharge? Insights from a salt marsh. Water Resources Research 51:4198–4207.

Wilson, A. M., and J. T. Morris. 2012. The influence of tidal forcing on groundwater flow and nutrient exchange in a salt marsh-dominated estuary. Biogeochemistry 108:27–38.

Wilson, A. M., and L. R. Gardner. 2006. Tidally driven groundwater flow and solute exchange in a marsh: Numerical simulations. Water Resources Research 42:W01405.

Xin, P., G. Jin, L. Li, and D. A. Barry. 2009. Effects of crab burrows on pore water flows in salt marshes. Advances in Water Resources 32:439–449.

Zinn, B., L. C. Meigs, C. F. Harvey, R. Haggerty, W. J. Peplinski, and C. F. Von Schwerin. 2004. Experimental visualization of solute transport and mass transfer processes in two-dimensional conductivity fields with connected regions of high conductivity. Environmental Science and Technology 38:3916–3926.